FMGM 2015 – PM Dight (ed.)

doi:10.36487/ACG_rep/1508_60_Afana

Increasing reliability in terrestrial laser data for slope failure monitoring

A Afana *3D Laser Mapping Ltd, UK*

G Hunter *3D Laser Mapping Ltd, UK*

N Rosser *Durham University, UK*

J Williams *Durham University, UK*

R Hardy *Durham University, UK*

Abstract

Terrestrial laser scanning (TLS) has provided new capabilities for real-time slope failure monitoring. For the mining industry, the advantages of TLS are not limited to deformation monitoring but also include a wide range of geotechnical and surveying applications such as characterising rockfall, 3D rock mass structure, and delineating features. Precision, repeatability and accuracy are crucial for deformation measurement. However, TLS data is affected by local climatic variations, such as fluctuations in temperature, rainfall, humidity, irradiance, and ambient light conditions. This is widely observed in open pit mines where high ranges (>2 km), often high temperature gradients and extremes, and steep topography result in highly variable measurement quality. As such, diurnal variations in ranging precision from TLS systems in such locations can reach up to 30-40 millimetres in some cases.

A direct-Fourier transformation method applied to sequentially captured time-series of TLS data is proposed to overcome such variability. By modelling diurnal fluctuations in range from independently monitored environmental variables, it is possible to estimate the frequency and phase characteristics of these effects. Discrimination between deformation and environmentally modulated cyclicity is achieved by modelling out trends in the TLS data. Results contribute to improving the precision of slope failure warning systems as a tool to enhance safety procedures for sustainable mining activities.

1 Introduction

In the last decade, terrestrial laser scanners (TLSs) have emerged as one of the key potential tools for 3D spatial data acquisition. In surveying and field measurement, TLS ability as a fast and accurate tool to capture 3D variations at high spatial resolution of 1 millimetre is one of the main benefits to consider, mainly in mining industry for deformation monitoring (Jaboyedoff et al. 2012) and safety warning systems. 3D variations in the terrain can be detected by comparing sequential scans. However, under real field conditions (e.g. variable local climate conditions), the precision of the TLS is not well known. This paper discusses issues influencing the feasibility of TLS systems for reliability measurements for deformation monitoring within real mining operation conditions.

The first output of the TLS system is 3D spatial data structure, widely known as a 'point cloud'. Registration of the point cloud (i.e. the process of geo-referencing two point clouds in one reference system) is performed either automatically or using control points (i.e. targets). The automatic registration of the point clouds without the use of targets is an area of increasing interest (Bae & Lichti 2004) and different models have been proposed (Tournas & Tsakiri 2008; Theiler & Chindler 2012). However, precision of these approaches is a matter of debate (Altuntas & Yilidz 2013) and targets registration (i.e. geo-referencing), if well applied, is still a reliable accurate approach. The target registration technique is based on placing artificial targets in the scene and identifying them in different scans. In the present work, SiteMonitor software (i.e. highly specialised software for slope failure monitoring) from 3D Laser Mapping was used for data acquisition and point clouds registration was performed using targets approach.

In mining, TLS is being widely introduced as a system of range, speed and resolution to align scales and geometry of the hillslope, giving rise to a new generation of slope failure and warning systems. Abellán et al. (2009) analysed precursory displacement with TLS and concluded that small precursory displacement could be hampered by the scanners own errors. Searching for sources of errors in field measurements is crucial for a more reliable TLS data capturing and processing. These sources of error may vary between instrument error, man-made error (e.g. surveying and processing errors), and weather-related errors that should be taken into account a priori to analysis process. Critically, efficiency and reliability of safety-critical warning systems is measured at millimetric scale of variations.

The main contribution of this paper is to highlight and identify sources of errors that may hamper the use of TLS for slope failure monitoring. Working across several monitoring datasets acquired by TLS systems in various large open pits, a clear cyclic behaviour was observed for average displacement of discrete monitored slopes. These observations provided a clear motivation for the present study, which basically aimed at studying the role of local climatic conditions on TLS data reliability for slope stability and failure monitoring. This paper addresses two main objectives: Analysing the temperature variability as a surrogate to local climate conditions to explain the cyclic behaviour in TLS data; and estimating the bias induced in TLS data by the variability of local temperature.

2 Methodology

A quick visual inspection of the data confirmed that the cyclic pattern corresponds to diurnal variations, which if plotted against corresponding air temperature measurements provided an interchangeable pattern between both components (Figure 1). The diurnal variation (a cyclic behaviour) in our data is assumed to be widely attributed to daily temperature (*t*) variations, in which the peaks and troughs of the cycle are aperiodic and widely related to minimum and maximum *t*, respectively. Such behaviour was observed in different data from various mines, where the diurnal variations in apparent deformation can reach up to 30-40 mm. Hence, our initial hypothesis estimates that air temperature plays a key role as a controlling factor of range measurements from TLS. A higher variation in temperature generates a greater variation in range and hence apparent displacement.

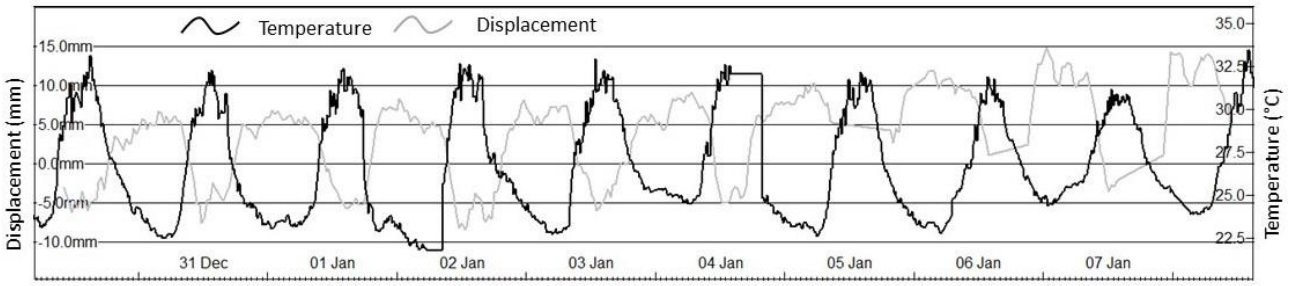

Figure 1 Displacement change through time against daily temperature variations in one of the analysed locations plotted using SiteMonitor safety system

2.1 Fast fourier transformation

In general, the time-series behaviour observed is understood as the displacement variation in TLS data, with absence of local errors, is stationary and is believed to be attributed to diurnal temperature variations. If the data is stationary, the fast fourier transformation (FFT) filters could be used to identify the general pattern in the data. The FFT filters provide accurate information about the frequency content of the data, which is used for removal of noise (Diodato & Bellochi 2011) and then to quantify the frequency domain. However, FFT assumes that the noise is also stationary, which in some cases may deviate; therefore, the non-stationarity prevails and the FFT application cannot be completed. In this case, the data should be corrected for longer-term variability, before completing the FFT. In order to secure stationarity, trend and seasonality were first estimated and then a simple subtraction removes these components from the original data. Later, residuals were evaluated using a Harmonic Autocorrelation Function (ACF).

Figure 1 confirms our data as stationary. The model used here to analyse the time-series contains a temperature trend, a cyclic trend (i.e. seasonality) and a residual. If we assume t is temperature, X_t is time series of displacement and T_t is trend function of temperature, an additive model to fit is defined as:

$$X_t = T_t + S_t + e_t \quad (1)$$

where:

S_t = seasonal component and represent the diurnal variation t.

e_t = error and residual.

T_t and S_t in Equation 1 are periodic functions which are approximated by two finite Fourier series, the first having seasonal harmonics and the second having a diurnal signal (Vinikov et al. 2006). Transformation of Equation 1 to first Fourier frequency is achieved by:

$$\text{Log}\,(X_t) = \alpha 0 + \alpha 1 t + \alpha 2 t^2 + \beta\cos(2\pi/f) + \Upsilon\sin(2\pi/f) + e_t \quad (2)$$

where:

α0, α1, α2 = constants.

f = diurnal data frequency.

β = amplitude of the cosine and sine waves, respectively.

In order to evaluate the trend and seasonality, if present, in time-series data a decomposition process is performed based on a simple moving average or a non-parametric regression technique (R Core Team 2015) if data shows seasonality. Original and final datasets as well as all the analysis process were handled in 'R' (http://cran.r-project.org).

3 Data

This study was carried out on data obtained from constant monitoring at PVDC-Barrick located in the Dominican Republic, approximately 100 kilometres northwest of the capital city of Santo Domingo.

Data acquisition was performed using a Riegl VZ-4000 scanner , which has a maximum range of 4,000 m, a beam divergence of 0.15 mrad (corresponding to 15 mm increase of beam width per 100 m of range), and an accuracy and precision of 15 and 10 mm, respectively. A scanning frequency every 2 hours was established for a period of about four months which extends between 25 April and 7 August 2014, totalling 675 scans. However, due to temporary power outages, there were some gaps in the data capturing, but these were limited to periods of only a few hours.

Average range displacement, hereinafter referred to as displacement, was estimated using SiteMonitor software. The frequency of data acquisition was established at 2 hours providing 12 scans per day. Figure 2 shows the resulting point cloud that covers the monitored area and the selected areas for analysis undertaken here. In total, four monitoring areas at different ranges from the TLS position were selected for analysis, each of which represent a vertical cut slope or bench wall. The selection of the four areas was merely to provide a representation of the wider monitored area, and at the same time reflected those areas best covered within the TLS field-of-view (i.e. vertical walls perpendicular the line-of-sight of the scanner).

Alignment of the different point clouds from TLS data was performed based on fixed target registration on each scan. This approach was adapted to provide millimetric registration accuracy between the consecutive scans. Five targets of 1 × 1 m dimension have been used and located at distances ranging between 305 m to 835 m. The registration process derives a range correct factor (RCF) and a tilt transformation matrix that rotates and scales consecutive scans to obtain the *real* position of the scanned objects. The RCF estimates the difference between two targets readings and provides a value that should compensates the effects of atmospheric variations. However, the response of the target material to local climatic variations is dissimilar to the rock face, leading to millimetre-scale variations as manifest in the diurnal variations in the

displacement readings, which motivates this study. Here, we seek to model this variation which is otherwise impossible to remove.

For the study period, temperature data was obtained from a local weather station within the mine, located about 5 m from the scanner position. An ideal estimation of temperature variation in relation to slope displacement required the presence of the measuring sensor near to the scanned area. However, this was impossible because of infrastructure availability and the mining activities within the monitoring areas. Hence, we assumed a similar distribution of air temperature throughout the monitoring pit, as the four select walls are all of a north-east facing aspect (Figure 2).

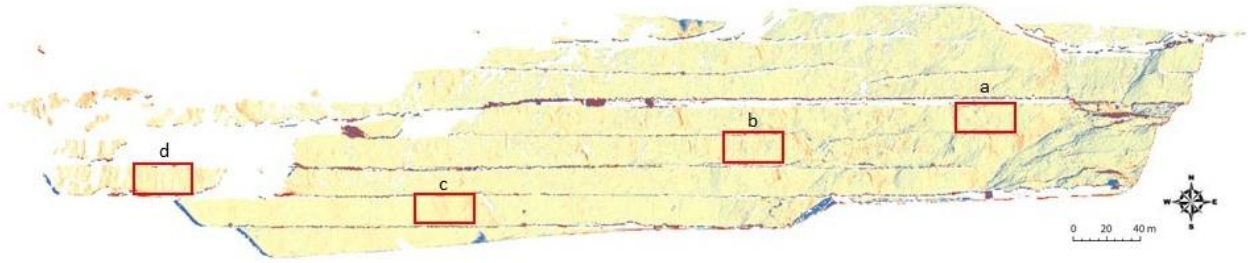

Figure 2 Location and distribution of the analysed areas within studied pit at PVDC-Barrick, Dominican Republic. Locations a, b, c, and d corresponds to ranges at 350, 500, 700 and 1,100 m, respectively

The original temperature series was collected at 10 minute intervals, which was transformed to a running average at 30 minutes intervals. Visual inspection of temperature data (Figure 3) for the studied period suggests a relatively stationary series, evidenced by the consistent daily temperature variations experienced during this period of the year. The PVDC mine temperature, within this part of the year, is characterised by 8-10 C daily variations in temperature. However, analysis based on ACF revealed a non-stationary aspect mainly between 5 and 12 May 2014 (Figure 3). This behaviour seems to be atypical and the series stabilises for the following period. Hence, non-stationarity was removed by de-trending the original data using the method described above (Figure 3(b)).

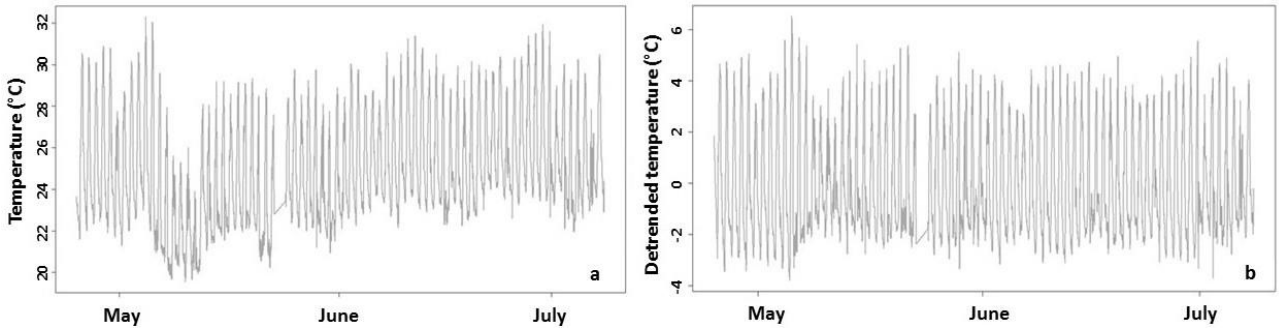

Figure 3 Time-series of (a) original temperature values and (b) de-trended values for the studied period

4 Results

Exploratory data analysis on the original temperature and displacement time series is aimed at identifying the temporal-pattern and corresponding variations in both datasets. Extremes and outliers have been identified using the bulk of the observations and then testing the degree to which any individual observation is likely to be an outlier (Statistics Netherlands 2010). Temperature data revealed no extremes or outliers. However, significant numbers of extremes and outliers in the displacement data were observed (Figure 4). That may correspond to anomalies resulting from the erroneous data (e.g. presence of machinery near to the area or any movements in the pillar, the targets used to align the point clouds, or from major rockfall events. A glance at the whole dataset reveals the presence of more than 30 rockfall

events of volumes between 2.1 and 105.2 m^3 occurred in this period, albeit limited to benches in the monitored area. However, stabilisation works to the slope within the monitored area took place between 26 April and 21 May 2014. This has directly affected the targets used in the alignment process of the point cloud, generating considerable errors in the acquired data. More than 35 scans distributed within this period have been removed from the analysis to overcome this effect.

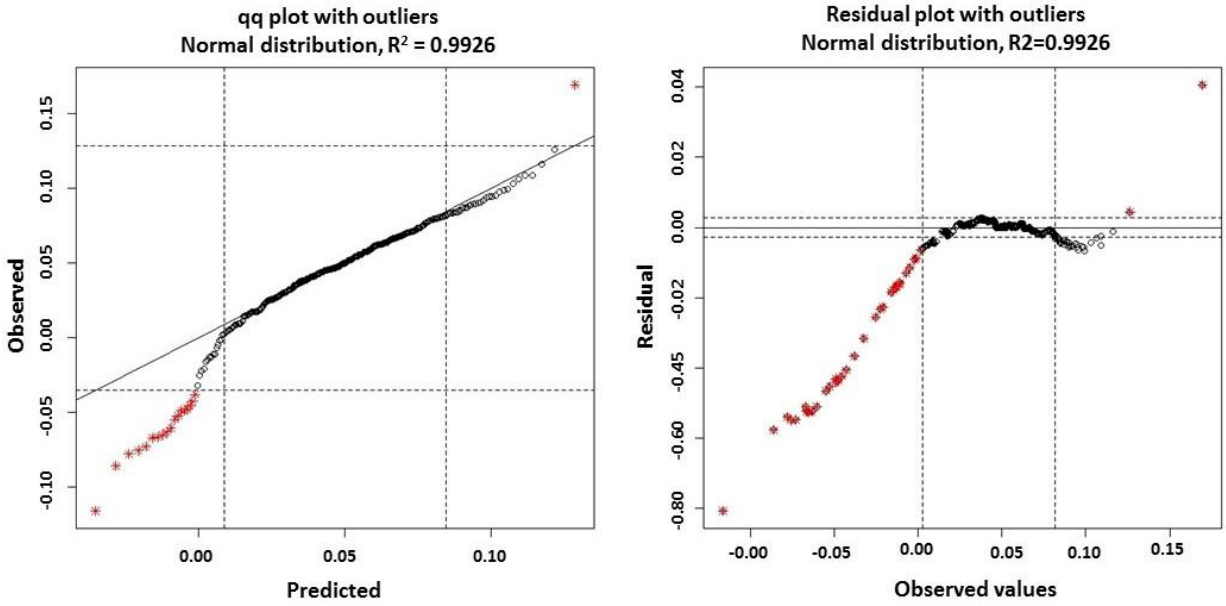

Figure 4 Outliers and extremes estimation in the data of Wall a located at 350 m from the scanner position. All crosses correspond to the anomalies in the grouped data

Table 1 shows basic summary statistics of central tendency and dispersion of the monitored locations. The first three locations show similar distributions for μ, σ, min and max. Wall (d) shows considerable dispersion values, which is attributed to the geometry of the location (i.e. high angle of incidence between the laser and the vector normal to the surface). Skewness for all locations was significantly low for Wall b, indicating a normal distribution for the bulk of the observations. The autocorrelation function (ACF) for each location and the residual distributions were evaluated for stationarity and homogeneity. Figure 5 shows the results of ACF and residuals in Wall a. The correlagram from the ACF shows a stationary series. The random residual distribution around the zero indicates no extreme drifts in data values through the monitored period. Similar results were also observed in Walls b, c, and d.

Table 1 Basic statistics of displacement of the four walls used in the analysis process. All units are in meters

Location	Mean (μ)	Standard deviation (σ)	Minimum (min)	Maximum (max)	Skewness (skew)
Wall a at 350 m	0.048	0.028	-0.042	0.125	-0.433
Wall b at 500 m	0.062	0.033	-0.044	0.166	-0.277
Wall c at 700 m	0.024	0.031	-0.066	0.117	-0.460
Wall d at 1,100 m	0.242	0.133	-0.174	0.636	-0.493

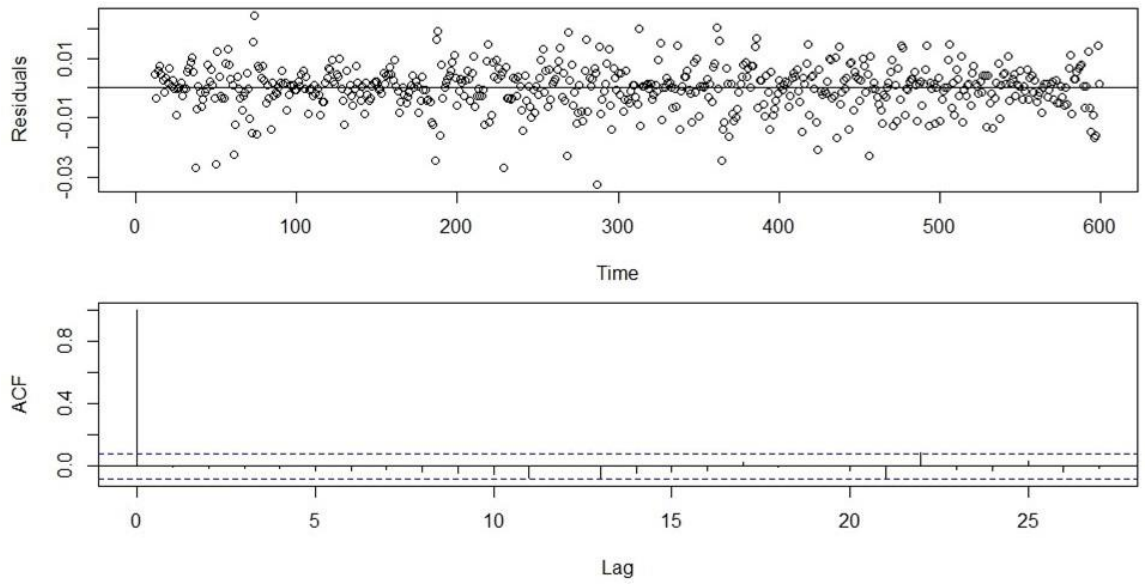

Figure 5 Residuals and autocorrelation function (ACF) for Wall a at PVDC mine. Scales are in metres

4.1 Time series modelling

The FFT analysis modelling of displacement (the dependent measurement) as a function of temperature (independent measurement) is summarised in Table 2. Results confirm an increasing effect of temperature range on diurnal displacement variations, showing a clear increase in the R^2 values. In all the FFT analysis, the temperature component (T_t) was significant at each of the different ranges of the analysed walls. Likewise, the seasonal component (S_t) confirms the cyclic effect on the diurnal displacement variations. However, this effect is revealed to be increasingly significant with range, with the exception in Wall d. This behaviour is explained by the targets' position and range to the scanner, which are used to estimate the range correction factor (RCF). In the analysed project, five targets have been used which are located at ranges that extend from 305 to 835 m. The final RCF is the average from all targets monitored. In this case, Wall d is located at 1,100 m and will receive an RCF that may not completely reflect the wider temperature effect. Hence, these results confirm the importance of the targets distribution within the monitored area in order to reflect real climatic variations. The higher the topographic contrasts in the mining operation area (e.g. strip mining or open pit mining), the greater the need for a good distribution of targets and monitoring sensors in order to reflect the local climatic conditions within the estimated RCF values.

Table 2 provides the percentage of diurnal variance in displacement as a function of temperature variation. As shown, the R^2 value obtained is significant for the four monitored locations and extends from 0.356 to 0.410. These values underline two important aspects of the behaviour of the apparent diurnal variation in displacement. First, variations in displacement increase proportionally in relation to the distance from the TLS position; the higher the range or object distance to the TLS the greater the diurnal variations. However, in large open pit mines (i.e. >2 km), high temperature variations within the monitoring areas also may lead to unpredictable variations in relation to diurnal displacement. Hence, both the conditions of mining operation (e.g. strip mining or open pit mining) as well as range values should be taken into account in understanding the variations of diurnal displacement with range. Second, although temperature seems to correlate well with displacement variations (Figure 1), it only explains part of the diurnal displacement variations, and other local factors could provide more insights on this behaviour.

Table 2 FFT modelling using average displacement against temperature at the four analysed location in PVDC mine

Location	Component	Intercept, p, t	R^2, *p*
Wall a at 350 m	Intercept	1.999, 3738.9, 2e-16	0.316, 7.6e-14
	T_t	-0.002, -7.479, 2.8e-09	
	S_t	0.468, 2.94, 0.003	
Wall b at 500 m	Intercept	1.999, 3155.961, 2e-16	0.351, 2.2e-16
	T_t	-0.002, -7.742, 4.31e-14	
	S_t	0.369, 4.233, 2.67e-05	
Wall c at 700 m	Intercept	2.000, 3895.924, 2e-16	0.363, 2.2e-16
	T_t	-0.001, -5.606, 3.1e-08	
	S_t	0.377, 7.076, 4.1e-12	
Wall d at 1,100	Intercept	1.995, 801.448, 2e-16	0.410, 2.2e-16
	T_t	-0.008, -7.523, 1.9e-13	
	S_t	0.267, 2.727, 0.006	

Factors such as irradiance, humidity, rainfall and ambient light conditions can play a major role and a more direct effect on the ranging precision. Irradiance is the radiant flux transmitted or received by a surface and indicates how much power incident upon the surface is emitted or reflected. This is a more sensitive parameter than temperature because it takes into account reflectance properties of the surface (e.g. brightness and material type, object geometry), which effect directly the reflected laser pulse (Lichti et al. 2002; Soudarissanane et al. 2009).

Figure 6 shows the original data and the fitted model of the FFT analysis for the diurnal displacement series of the four locations consider here. In the original time-series, the highest displacement variations are registered at location Wall d, whereas the smallest are at locations Walls a and b. The maximum and minimums as well as the general trend in the original time-series is attributed to location geometry (object location in relation the angle of incidence of the laser pulse), range (the higher the range the higher the noise), and to the instrument error (laser beam divergence in relation to distance). Also, it is worth underlining that in the present FFT analysis we tried to avoid data filtering in order to maintain the real data structure as received by the technical staff in the mine. This should reflect major and minor events (e.g. rockfall, deformation etc.) during mining operations.

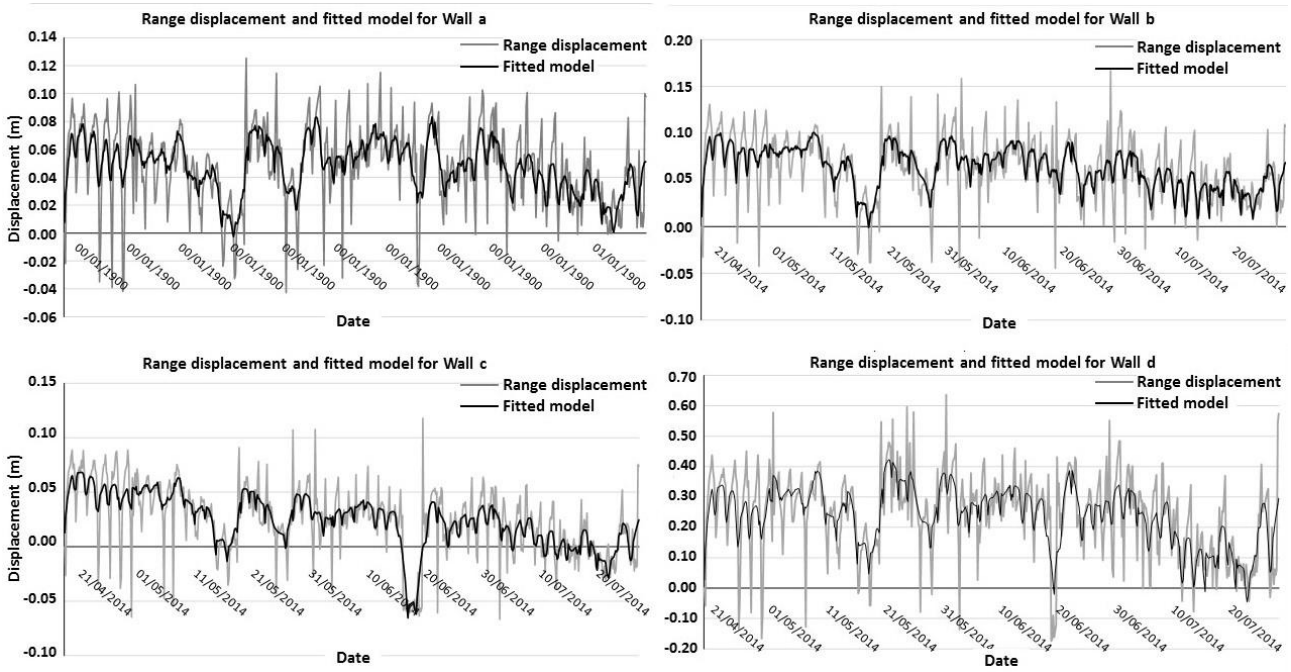

Figure 6 Time-series of average displacement for the four analysed walls and fitted models from the FFT

Finally, Figure 7 shows a dataset for one week, with the modelling range displacement from the FFT analysis. The results show a clear decrease in displacement variations for the analysed period from 20 mm to less than 5 mm. However, the cyclic pattern is still perceived in the displacement curve (Figure 7) highlighting the presence of more than one controlling factor in the diurnal behaviour. While temperature explains up to 75% of the diurnal variations, analysing a combination of local climatic factors (e.g. temperature, rainfall, humidity, irradiance and ambient light conditions) may provide deeper insight and better interpretation of the cyclicity in the displacement curve. Nevertheless, in open pit mining, and based on rock structure components, a 5 mm noise seems to be a reasonable approximation for reliable alarming.

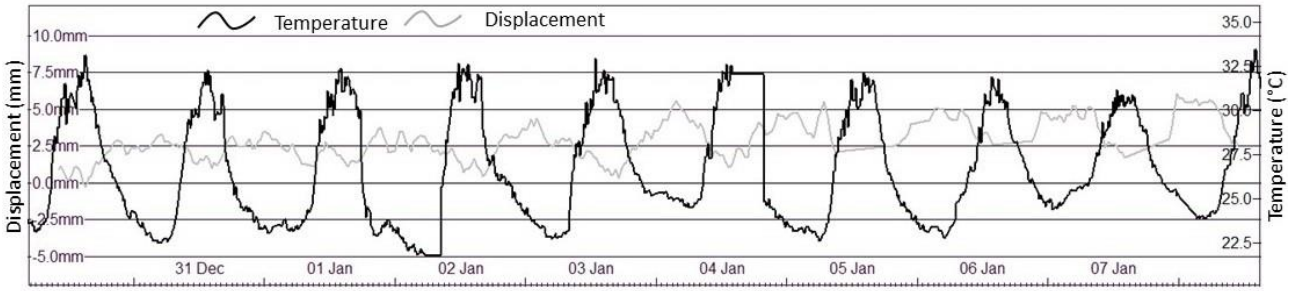

Figure 7 Modelled range displacement change by the FFT approach through time against daily temperature variations in one of the analysed locations plotted using SiteMonitor safety system

4.2 Quantification of bias diurnal variation by range

The fitted model applied from Equation 2 to the four time-series shows a good approximation to the original data. Most of the diurnal variations are well described in the proposed approach. However, it seems that the model fails to emulate the magnitude of the peaks and troughs of each cyclic in the time-series. Again, modelling the displacement variations by a unique variable (T_t), in this case, could provide partial explanation of the cyclic behaviour in data captured by TLS. Moreover, the fitted models provided smaller frequency displacement rates, where daily variations were reduced to scales of ± 3 cm.

Such reduced frequencies are more likely to approximate similar results obtained from other monitoring sensors in the area (e.g. prisms and total stations). This increasing in data reliability directly allows introducing a more consistent threshold that copes with the geotechnical standards of the mine for warning alarming in the monitoring plan.

The total diurnal variation in displacement for each monitored area is reflected by the global standard deviation (σ). Assuming that this variation is directly proportional to range from the TLS position, the bias (δ) introduced by T_t can be deduced directly from the difference between original and fitted model variations (σ'):

$$\delta = \sigma - \sigma' \tag{3}$$

Figure 8 shows δ values for the four monitored walls plotted against range. The four locations were used to generate a linear fit (δ1) of 0.83 R^2 providing a bias of 0.004 m/100 m, which is attributed directly to the T_t component. However, when only the first three locations was used to estimate the fit, the noise was reduced to 0.0004 m/100 m. Importance of these values reside in the degree of the acceptable noise that should be added at the initial threshold in order to establish a reliable alarming system within the mine. Importantly, these results confirm that temperature variations on TLS data aligned by artificial targets could vary in relation to range values. This requires special attention from the geotechnical staff at the mine to take into account such variations. A safety-critical warning system requires strict identification of all parameters involved directly in providing the most accurate threshold to provide the correct slope failure measurement and alarming. Future work on TLS data variations is needed to quantify the direct local climatic parameters involved and their effect in relation to range or distance values of the TLS position, including minimum and maximum if possible.

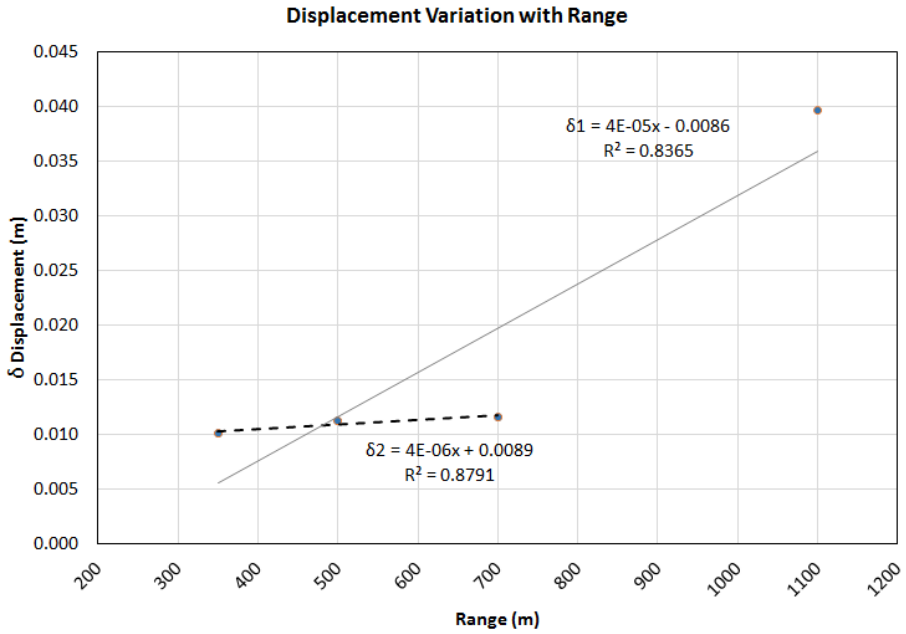

Figure 8 A linear fit for bias (δ) values estimated with two groups of data. δ1 is for Walls a, b, c and d, whereas δ2 is for Walls a, b and c

5 Conclusion

This paper describes a new technique for investigating TLS data bias, notably in ranging precision, in relation to local climatic variations. The present work was limited to considering air temperature variations. TLS data, when aligned by artificial targets, is usually subjected to artificial variations and highly variable measurement quality that may reduce reliability in the alarming thresholds implied within safety warning systems. In open pit mines where high ranges (>2 km) and steep topography, such diurnal variations can reach up to 30-40 millimetres in some cases.

Identifying are temperature as the key component that affects TLS data variability, a FFT model approach was applied to a time-series data captured at different ranges from the TLS system. The FFT model allows the quantification of the total bias generated at each location providing a better approximation of a more reliable threshold to be implemented in safety warning systems in the mine. Likewise, diurnal variations in TLS data modelled only by temperature component, as surrogate for all influential local climatic variations, have explained only 30-40% of the total variations. These results emphasise a crucial need for more work that should take into account other local climatic components to explain the complete diurnal variations and the cyclic behaviour in TLS data.

Acknowledgement

We thank PVDC-Barrick Mine for providing all necessary data and collaboration to complete this study. The study was funded by the Knowledge Transfer Partner (KTP) project between Durham University and 3D Laser Mapping Ltd. (KTP8878), and support from the UK NERC, TSB and EPSRC.

References

Abellán, A, Jaboyedoff, M, Oppikofer, T & Vilaplana, J 2009, 'Detection of millimetric deformation using a terrestrial laser scanner: experiment and application to a rockfall event', *Natural Hazards and Earth System Science*, vol. 9**,** pp. 365-372.

Altuntas, C & Yildiz, F 2013, 'Point cloud registration and virtual realization of large scale and more complex historical structures', *ISPRS-International Archives of the Photogrammetry, Remote Sensing and Spatial Information Sciences*, vol. 1, no. 2, pp. 13-18.

Bae, KH & Lichti, DD 2004, 'Automated registration of unorganised point clouds from terrestrial laser scanners', in O Altan (ed.), *International Archives of Photogrammetry and Remote Sensing (vol. XXXV: Part B5), Proceedings of the ISPRS Working Group V/2*, International Society for Photogrammetry and Remote Sensing, pp. 222-227.

Diodato, N & Bellocchi, G 2011, 'How predictable are temperature-series undergoing noise-controlled dynamics in the Mediterranean, *Nature Precedings*, 9 p.

Jaboyedoff, M, Oppikofer, T, Abellán, A, Derron, MH, Loye, A, Metzger, R & Pedrazzini, A 2012, 'Use of LIDAR in landslide investigations: a review', *Natural hazards*, vol. 61, pp. 5-28.

Lichti, D, Gordon, S & Stewart, M 2002, 'Ground-based laser scanners: operation, systems and applications', *Geomatica*, vol. 56, no. 1, pp. 21-33.

R Core Team 2015*, R: A language and environment for statistical computing,* Reference Index, R Foundation for Statistical Computing, Vienna, 3604 p.

Soudarissanane, S, Lindenbergh, R, Menenti, M & Teunissen, P 2009, 'Incidence angle influence on the quality of terrestrial laser scanning points', *ISPRS Workshop Laser Scanning*, 6 p.

Statistics Netherlands 2010, *Distribution based outlier detection for univariate data*, Technical Report 10003, prepared by MPJ Van der Loo, Heerlen.

Theiler, PW & Schindler, K 2012, 'Automatic registration of terrestrial laser scanner point clouds using natural planar surfaces', in M Shortis, N Paparoditis & C Mallet (eds), *Proceedings of the ISPRS Annals of the Photogrammetry, Remote Sensing and Spatial Information Sciences Congress* (vol. I-3), International Society for Photogrammetry and Remote Sensing, pp. 173-178.

Tournas, E & Tsakiri, M 2008, 'Deformation monitoring based on terrestrial laser scanner point cloud registration', *Proceedings of the 13th FIG Symposium on Deformation Measurement and Analysis*, 10 p.

Vinikov, KY, Grody, NC, Robock, A, Stouffer, RJ, Jones, PD & Goldberg, MD 2006, 'Temperature trends at the surface and in the troposphere', *Journal of Geophysical Research*, vol. 111, no. D3.